Turbulent Flow in Channels in Terms of Local Turbulent Shear and Normal Stresses

Stuart W. Churchill and Christina Chan
Dept. of Chemical Engineering, University of Pennsylvania, Philadelphia, PA 19104

The local time-averaged velocity, the mixed-mean velocity, and the friction factor for fully turbulent flow between parallel plates and in round tubes and concentric circular annuli can be expressed in terms of integrals of the turbulent shear stress. The pressure distribution across a channel can similarly be expressed in terms of an integral of normal stresses. These formulations, which are simple and exact, can be integrated numerically using experimental data, computed values, or correlating equations for turbulent stresses. Their greatest merit, however, may arise from the insight they provide with respect to the contributions of the fluctuating components of the velocity. For example, for concentric circular annuli such a formulation identifies a difference between the locations of the maximum in the velocity and the zero in the total shear stress. This difference, which has been overlooked in most experimental and semitheoretical investigations, introduces an error of unknown but possibly significant magnitude into all of the results. It also precludes the application of the mixing-length, eddy viscosity and $k-\epsilon$ models.

Introduction

Until very recently most theoretical results for turbulent flow in channels have been based on the time-averaged equations of conservation. In the past few years some success has been attained in solving the time-dependent form of these expressions numerically using direct-digital, spectral, and pseudospectral methods. The results of the latter methodologies are promising in that they appear to be accurate and to provide greater precision and detail than may ever be possible experimentally. However, with current computing machinery and algorithms, such solutions, as illustrated by those of Kim et al. (1987) and Rutledge and Sleicher (1993) for fully developed flow between parallel plates at $b^+ = 180$ (or $Re \cong 11{,}500$) and of Lyons et al. (1991) for the same geometry at $b^+ = 150$ or ($Re \cong 9{,}000$), are limited to very simple geometries and very low Reynolds numbers (at the lower limit of fully turbulent flow). Some time may pass before solutions are attained for significantly greater rates of flow and more complex geometries. In any event, the results obtained by such predictive methods are equivalent in form to experimental data except for greater precision, frequency, and possible accuracy, in that they are discrete and provide no functionality. For that reason, time-averaged models can be expected to retain a useful role indefinitely in terms of providing a closed-form structure for correlation.

Time-averaging does of course result in the loss of some information as a tradeoff for the considerable simplification. This loss identified by the appearance of new unknown quantities such as $\overline{u'v'}$ in the equations of conservation for momentum. For fully developed flow between parallel plates and in round tubes, empirical algebraic models in terms of the eddy kinematic viscosity of Boussinesq (1877) or the mixing-length of Prandtl (1925) have represented $\overline{u'v'}$ with considerable success and thereby allowed solution of the time-averaged equations of conservation for the velocity distribution and the shear stress on the wall. For more complex geometries, semiempirical differential equations of conservation for the kinetic energy of turbulence k and the rate of dissipation of turbulence, ϵ, as well as for $\overline{u'v'}$ itself, have been utilized with mixed success.

The methods of prediction mentioned in the previous paragraph are not examined herein. Instead, a quantitative integral formulation is considered that in itself reveals more about the functionality than detailed numerical solutions.

Correspondence concerning this article should be addressed to S. W. Churchill.
Current address of C. Chan: E. I. du Pont Marshall Laboratory, 3500 Grays Ferry Road, Philadelphia, PA 19146.

While this integral formulation is not completely unknown (see, for example, Kampe de Fériet, 1948; Pai, 1953a,b; Kjellström and Hedberg, 1966), its usefulness has not generally been recognized. Particular attention is given herein to the continuing cost of that oversight in terms of the misinterpretation of experimental data and the derivation of invalid solutions.

In the interests of simplicity, the results herein are limited to fully developed, fully turbulent flow and invariant physical properties.

Smooth Parallel Plates

The somewhat idealized geometry of smooth parallel plates of infinite extent is chosen as a first example, again for reasons of simplicity. For this condition the time-averaged equations of conservation can be expressed in the following forms:

$$-\frac{\partial P}{\partial x}+\frac{d}{dy}\left(\mu\frac{du}{dy}-\rho\overline{u'v'}\right)=0 \tag{1}$$

$$-\frac{\partial P}{\partial y}-\frac{d}{dy}\left(\rho\overline{v'v'}\right)=0 \tag{2}$$

and

$$-\frac{d}{dy}\left(\rho\overline{w'v'}\right)=0. \tag{3}$$

The superbars designating time-averaged values of P and u have been dropped for simplicity, but those for the products of the fluctuating components of the velocity are retained for clarity.

Integration of Eqs. 2 and 3 with the postulate (well-confirmed experimentally) that $\overline{v'v'}$ and $\overline{w'v'}$ vanish at $y=0$ yields

$$P=P_w-\rho\overline{v'v'} \tag{4}$$

and

$$\overline{w'v'}=0. \tag{5}$$

This first integration has produced the valuable information that $\overline{w'v'}$ is exactly zero for all y and that the pressure is reduced from its value at the wall by an amount exactly equal to the local value of $\rho\overline{v'v'}$ ($\overline{v'v'}$ can be recognized as the square of the root-mean-square of v').

Since the right-most term of Eq. 2 is independent of x, it follows that $\partial P/\partial y$ is as well. Differentiation of $\partial P/\partial y$ with respect to x then leads to the conclusion that $\partial P/\partial x$ is a constant (invariant with respect to both x and y). Integrating Eq. 1 from $y=b$, the midplane between the plates, where, from symmetry, $\mu(du/dy)-\rho\overline{u'v'}=\tau$ is zero, then gives

$$(b-y)\left(-\frac{\partial P}{\partial x}\right)=\mu\frac{du}{dy}-\rho\overline{u'v'}. \tag{6}$$

Since from symmetry, du/dy is also zero at $y=b$, it follows that the turbulent shear stress, which is equal to $-\rho\overline{u'v'}$, must vanish at that point. It also follows from Eq. 6 that $u'v'$ must be negative for $0<y<b$.

From an overall force balance,

$$-\frac{\partial P}{\partial x}b=\tau_w. \tag{7}$$

Hence, Eq. 6 can also be expressed as

$$\left(1-\frac{y}{b}\right)\tau_w=\mu\frac{du}{dy}-\rho\overline{u'v'}, \tag{8}$$

or in dimensionless form as

$$1-\frac{y^+}{b^+}=\frac{du^+}{dy^+}+\phi^+. \tag{9}$$

Formal integration of Eq. 9 from $u^+=0$ at $y^+=0$ gives, after rearrangement, the following expression for the velocity distribution:

$$u^+=y^+\left(1-\frac{y^+}{2b^+}\right)-\int_0^{y^+}\phi^+\,dy^+. \tag{10}$$

It follows that

$$u_b^+=u_{\max}^+=\frac{b^+}{2}-b^+\int_0^1\phi^+d\left(\frac{y^+}{b^+}\right) \tag{11}$$

and that

$$u_m^+\equiv\int_0^1 u^+d\left(\frac{y^+}{b^+}\right)=\frac{b^+}{3}-\int_0^1\left[\int_0^{y^+}\phi^+dy^+\right]d\left(\frac{y^+}{b^+}\right). \tag{12}$$

By formally reversing the order of integration or integrating by parts, Eq. 12 can be reduced to

$$u_m^+=\frac{b^+}{3}-b^+\int_0^1\phi^+\left(1-\frac{y^+}{b^+}\right)d\left(\frac{y^+}{b^+}\right). \tag{13}$$

Equation 13 can also be expressed as

$$fRe=\frac{24}{1-3\int_0^1\phi^+(1-(y^+/b^+))d(y^+/b^+)}. \tag{14}$$

The dimensionless turbulent shear stress in Eqs. 9–14 is defined as

$$\phi^+=-\frac{\rho\overline{u'v'}}{\tau_\omega}. \tag{15}$$

This quantity can be recognized as the local turbulent shear stress as a fraction of the total shear stress on the wall. Since

$u'v'$ is negative for $0 \le y^+ \le b^+$, ϕ^+ is positive over that range. From Eq. 8 it follows that the fraction of the total shear stress at any point due to the turbulent fluctuations is

$$-\frac{\rho\overline{u'v'}}{\tau} = \frac{\phi^+}{1-(y/b)} \tag{16}$$

Kampe de Fériet (1948) apparently first derived the equivalent of Eqs. 10–13, but he did not analyze or pursue the consequences of these results.

Interpretation

As was to be expected, Eqs. 9–14 reduce to the well-known expressions for laminar flow when ϕ^+ is equated to zero. What is perhaps surprising is that the contributions of turbulence, as expressed by the integrals of Eqs. 10–14, are simply subtractive from the terms for purely laminar flow.

As is well known, u^+ is a function of y^+ and b^+ for fully turbulent flow, approaching a dependence on y^+ alone for $y^+ \ll b^+$ and a dependence on y^+/b^+ alone for $y^+ \to b^+$. It follows from Eq. 9 that ϕ^+ bears a one-to-one correspondence with u^+ and thereby is dependent on the same variables in general and in the two limits. Indeed, $\phi^+\{y^+, b^+\}$ can obviously be determined from $u^+\{y^+, b^+\}$ by means of Eq. 9. Differentiation of experimental data magnifies its uncertainty (see, for example, Churchill (1979), chaps. 5 and 6, and de Nevers (1966)). This magnification of error may account in part for the scarcity, as noted below, of specific correlating equations for $\phi^+\{y^+, b^+\}$ as compared to those for $u^+\{y^+, b^+\}$. Another explanation is the greater experimental difficulty of measuring $\overline{u'v'}$ as compared to u, and the lesser number of sets of such values.

Correlations

Churchill and Chan (1995), as an outgrowth of the current article, devised the following correlating equation for ϕ^+ for fully developed, fully turbulent flow between parallel plates ($b^+ > 180$):

$$\frac{1}{\phi^+} = \frac{1}{0.7}\left(\frac{10}{y^+}\right)^3 + \frac{1}{(1-(y^+/b^+))\left|e^{-2.5/y^+} - (2.5/b^+)(1+(4y^+/b^+))\right|} \tag{17}$$

Equation 17 is applicable for all y^+; it conforms to the presumed asymptotic behavior in the viscous sublayer near the wall ($y^+ < 5$), in the fully turbulent core near the wall ($30 < y^+ < 0.1b^+$), and in the region of the wake near the central plane ($0.5 < (y^+/b^+) \le 1$). As illustrated in Figures 1 and 2, ϕ^+, per Eq. 17, rises rapidly from zero at the wall, attains a maximum value of approximately $1-(10/b^+)^{1/2}$ at $(y^+/b^+) \cong (2.5/b^+)^{1/2}$ [or $y^+ \cong (2.5b^+)^{1/2}$], and then decreases almost linearly to zero at the central plane ($y^+ = b^+$).

Equation 17 is an alternative to corresponding correlating equations for the distribution of the time-mean velocity, the mixing length, and the eddy viscosity. The greater complexity of Eq. 17 relative to the more familiar ones for the velocity,

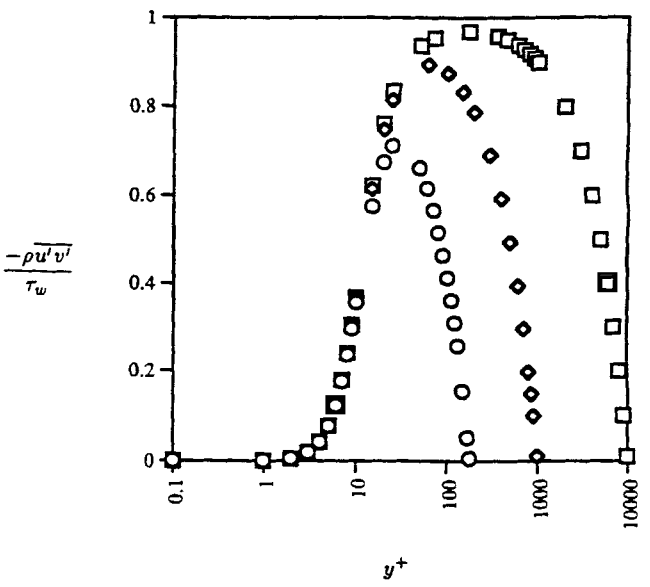

Figure 1. Dimensionless turbulent shear stress as a function of y^+ according to Eq. 17.

○ = b^+/180; ◇ = 1,000; □ = 10,000.

the eddy viscosity, and the mixing length is a consequence of the incorporation of the theoretically based behavior for all three regimes. For example, the exponential term by itself corresponds to the semilogarithmic regime of the velocity distribution and the quasilinear regimes of the eddy viscosity and the mixing length. Equation 17 actually incorporates one less empirical constant and one less functional approximation than the analogous expression of Churchill and Chan (1994)

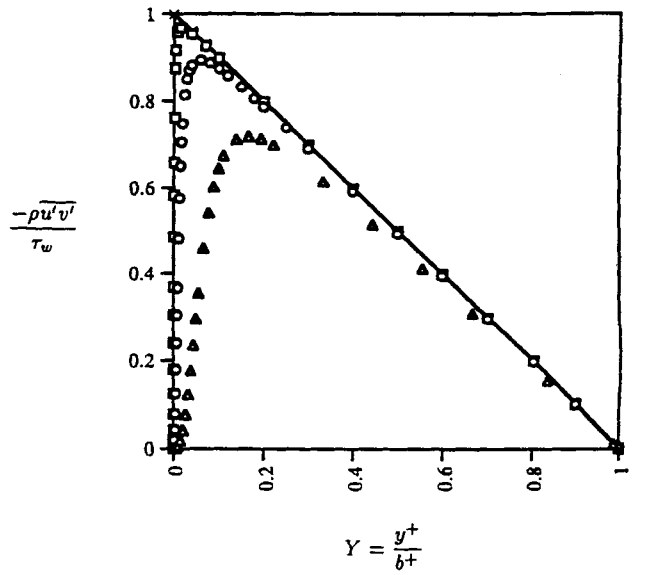

Figure 2. Dimensionless turbulent shear stress as a function of y/b according to Eq. 17.

b^+; △ = 180; ○ = 1,000; □ = 10,000; $-(\rho\overline{u'v'})/\tau_w = 1-(y/b)$.

for u^+. The coefficient 0.7 and the exponent 3 were chosen on the basis of numerical simulations of turbulent flow near a wall, while the coefficients 2.5 and 4 were chosen on the basis of empirical representations for the velocity distribution in the turbulent core near the wall and near the central plane, respectively.

Equation 9 reveals the simple relationship between du^+/dy^+ and ϕ^+. The corresponding relationships of ϕ^+ with the eddy kinematic viscosity and the mixing length are

$$\frac{\nu_t}{\nu} = \frac{\phi^+}{1-(y^+/b^+)-\phi^+} \tag{18}$$

and

$$(l^+)^2 = \frac{\phi^+}{[1-(y^+/b^+)-\phi^+]^2}. \tag{19}$$

Equation 17 can be used to evaluate u^+, u_b^+, u_m^+, and f by numerical integration for any specified value of b^+ greater than 150, which is the approximate lower limit of fully turbulent flow between parallel plates.

Pai (1953a) appears to be the only prior investigator to propose a correlating equation for $\overline{u'v'}$ for flow between parallel plates. First, he repeated the derivation of Kampe de Fériet (1948). Then he devised the following empirical expression to represent the experimental velocity distribution of Laufer (1951) for $bu_{max}/\nu = 12{,}300$:

$$\frac{u}{u_{max}} = 1-0.3293\left(1-\frac{y}{b}\right)^2 - 0.6707\left(1-\frac{y}{b}\right)^3. \tag{20}$$

By substituting Eq. 20 in the equivalent of Eqs. 9 and 11 he derived an expression for $\phi^+\{y/b\}$, and in turn from Eq. 13 an expression for the friction factor. He compares his expressions for u/u_{max} and ϕ^+ with the experimental data of Laufer (1951), but does not evaluate numerically or critique his expression for f. Despite the superficial agreement that he demonstrates, his expressions for u/u_{max}, ϕ^+, and f are functionally inadequate. In particular, Eq. 20 fails to conform to the known dependence of u^+ on y^+ alone for $y^+ < 0.1b^+$. An immediate consequence is the restriction of Eq. 20 to the single rate of flow corresponding to $bu_{max}/\nu = 12{,}300$. His expression for ϕ^+ has directly related shortcomings, and that for f erroneously demonstrates an inverse proportionality to $(b^+)^2$ as in laminar flow.

Smooth Round Tubes

The expressions for smooth round tubes are closely analogous to those for smooth parallel plates and hence will be presented only insofar as they differ.

The time-averaged equations of conservation for fully developed flow can be expressed in the following forms:

$$-\frac{\partial P}{\partial r} - \frac{1}{r}\frac{d}{dr}(\rho r\overline{u_r'u_r'}) + \frac{\rho\overline{u_\theta'u_\theta'}}{r} = 0 \tag{21}$$

$$\frac{1}{r}\frac{d}{dr}(r\overline{u_r'u_\theta'}) + \frac{\overline{u_r'u_\theta'}}{r} = 0 \tag{22}$$

and

$$-\frac{\partial P}{\partial z} + \frac{1}{r}\frac{d}{dr}\left(\mu r\frac{du_z}{dr} - \rho r\overline{u_r'u_z'}\right) = 0. \tag{23}$$

The same process of analysis and integration as for parallel plates yields

$$P = P_w - \rho\overline{u_r'u_r'} - \rho\int_r^a (\overline{u_\theta'u_\theta'} - \overline{u_r'u_r'})\frac{dr}{r} \tag{24}$$

$$\overline{u_r'u_\theta'} = 0 \tag{25}$$

and

$$\frac{r}{2}\left(-\frac{\partial P}{\partial z}\right) = -\mu\frac{du_z}{dr} + \rho\overline{u_r'u_z'}. \tag{26}$$

The cross-product $\overline{u_r'u_\theta'}$, when multiplied by ρ, can in this geometry be recognized at once as the Coriolis force. It is seen from Eq. 25 to be zero at all radii. The contributions to the radial variation in pressure that appear as the first and second terms of the integral of Eq. 24 are due to the centrifugal force and curvature, respectively. The turbulent shear stress $\rho\overline{u_r'u_z'}$ is seen from Eq. 26 to be zero at the centerline.

Equation 26 can be rewritten in terms of the shear stress on the wall as

$$\frac{r}{a}\tau_w = -\mu\frac{du_z}{dr} + \rho\overline{u_r'u_z'}. \tag{27}$$

If, for purposes of comparison, u_z were replaced by u, a by b, r by $b-y$, and $\overline{u_r'u_z'}$ by $-\overline{u'v'}$, Eq. 27 would become identical to Eq. 8. It follows that Eqs. 9–11 are directly applicable to a round tube if a^+ is substituted for b^+. However, for round tubes

$$u_m = \int_0^1 ud\left(\frac{r}{a}\right)^2 \tag{28}$$

and Eqs. 13 and 14 are replaced by

$$u_m^+ = \frac{a^+}{4} - \frac{a^+}{3}\int_0^1 \phi^+ d\left(\frac{r}{a}\right)^3 \tag{29}$$

and

$$fRe = \frac{16}{1-\frac{4}{3}\int_0^1 \phi^+ d\left(\frac{r}{a}\right)^3}. \tag{30}$$

Insofar as the extended analogy of MacLeod (see Churchill (1990) or Churchill (1994), chap. 10) is valid, Eq. 17 is directly applicable to round tubes if a^+ is substituted for b^+.

The only prior application of the integral formulation to round tubes is also apparently due to Pai (1953b). His derivation is equivalent to that herein except that he erroneously omitted a factor of r/a in the equivalent of Eq. 29. His proposed empirical expressions for the distributions of u/u_m and ϕ^+ differ from those of his for parallel plates, but have similar shortcomings. Hence, they will not be reproduced or discussed further herein.

Equation 17 with a^+ substituted for b^+ can be used with Eqs. 10, 11, 29 and 30 to determine $u^+\{y^+\}$, u_a^+, u_m^+, and fRe for round tubes for any specified $a^+ \geq 150$. However, just as for parallel plates, the greatest value of the expressions previously derived for round tubes is perhaps the direct demonstration of the contribution of the turbulent fluctuations to the variation of the pressure and time-mean velocity across the channel, and to the friction factor. The more complex expressions that follow for concentric circular annuli have additional value and functional significance.

Concentric Circular Annuli

Equations 21–23 are directly applicable for a concentric circular annulus. Equation 25 is also valid, and Eq. 24 is adaptable if P_w and a are designated as either P_{w1} and a_1 or P_{w2} and a_2. Equation 26 is not applicable since the implied boundary condition of $(du_z/dr) = 0$ and $\overline{u_r'u_z'} = 0$ at $r = 0$ is no longer appropriate. Instead, integrating Eq. 23 from $a_{\max}$, the unknown radius at which u_z is a maximum and du_z/dr is zero, yields

$$-\frac{\partial P}{\partial z}\left(\frac{a_{\max}^2 - r^2}{2}\right) = \rho a_{\max}(\overline{u_r'u_z'})_{a_{\max}} - \rho r\overline{u_r'u_z'} + \mu r\frac{du}{dr}. \quad (31)$$

The subscript m on the time-mean velocity has been dropped in Eq. 31 and thereafter in the interest of simplicity.

Alternatively, integrating Eq. 23 from a_0, the unknown radius at which the total shear stress is zero, yields

$$-\frac{\partial P}{\partial z}\left(\frac{a_0^2 - r^2}{2}\right) = \rho a_0(\overline{u_r'u_z'})_{a_0} - \rho r\overline{u_r'u_z'} - \mu a_0\left(\frac{du}{dr}\right)_{a_0} + \mu r\frac{du}{dr}. \quad (32)$$

The total shear stress (here arbitrarily defined to be positive for $r < a_0$) can be expressed as

$$\tau = \mu\frac{du}{dr} - \rho\overline{u_r'u_z'}. \quad (33)$$

Since this quantity is by definition zero at $r = a_0$,

$$\mu\left(\frac{du}{dr}\right)_{a_0} - \rho(\overline{u_r'u_z'})_{a_0} = 0 \quad (34)$$

and Eq. 32 can be reduced to

$$-\frac{\partial P}{\partial z}\left(\frac{a_0^2 - r^2}{2}\right) = -\rho r\overline{u_r'u_z'} + \mu r\frac{du}{dr}. \quad (35)$$

Specializing Eq. 35 for $a_{\max}$ or subtracting Eq. 35 from Eq. 31, produces

$$-\frac{\partial P}{\partial z}\left(\frac{a_{\max}^2 - a_0^2}{2}\right) = \rho a_{\max}(\overline{u_r'u_z'})_{a_{\max}}. \quad (36)$$

Equation 36 can be considered to be the analog of the condition of zero turbulent shear stress at $y = b$ for parallel plates and at $r = 0$ for round tubes.

It follows from Eq. 36 that for laminar flow, for which $\overline{u_r'u_z'} = 0$ at all r, the maximum in the velocity and the zero in the total shear stress are coincident in an annulus just as they are for both laminar and turbulent flow in round tubes and between parallel plates. On the other hand, these locations must differ in turbulent flow in an annulus if $\overline{u_r'u_z'}$ is finite at the maximum in the velocity. Direct measurements of $\overline{u_r'u_z'}$ of sufficient accuracy to determine whether or not $(\overline{u_r'u_z'})_{a_{\max}}$ is finite are limited, but, as discussed below, definitive measurements of time-mean quantities that distinguish a_0 and $a_{\max}$ have been obtained.

Integrating Eq. 35 from the outer radius, a_2 gives, upon rearrangement,

$$u = \frac{1}{\mu}\left(-\frac{\partial P}{\partial z}\right)\left(\frac{a_2^2 - r^2}{4} - \frac{a_0^2}{2}\ln\left\{\frac{a_2}{r}\right\}\right) - \frac{\rho}{\mu}\int_r^{a_2}\overline{u_r'u_z'}dr. \quad (37)$$

Specializing Eq. 37 for the inner radius a_1, where $u = 0$, leads to

$$\left(\frac{a_0}{a_1}\right)^2 = \frac{\left(\frac{a_2}{a_1}\right)^2 - 1 - \frac{4\rho}{a_1^2(-\partial P/\partial z)}\int_{a_1}^{a_2}\overline{u_r'u_z'}dr}{2\ln\left\{\frac{a_2}{a_1}\right\}}. \quad (38)$$

Eliminating a_0 between Eqs. 37 and 38 then results in

$$u = \frac{1}{4\mu}\left(-\frac{\partial P}{\partial z}\right)\left[a_2^2 - r^2 - (a_2^2 - a_1^2)\left(\frac{\ln\left\{\frac{a_2}{r}\right\}}{\ln\left\{\frac{a_2}{a_1}\right\}}\right)\right] + \frac{\rho}{\mu}\left(\frac{\ln\left\{\frac{a_2}{r}\right\}}{\ln\left\{\frac{a_2}{a_1}\right\}}\right)\int_{a_1}^{a_2}\overline{u_r'u_z'}dr - \frac{\rho}{\mu}\int_r^{a_2}\overline{u_r'u_z'}dr. \quad (39)$$

Finally, integrating over the entire annulus and dividing by the cross-sectional area gives

$$u_m = \frac{1}{8\mu}\left(-\frac{\partial P}{\partial z}\right)\left[a_2^2 + a_1^2 - \frac{a_2^2 - a_1^2}{\ln\left\{\frac{a_2}{a_1}\right\}}\right] + \frac{\frac{\rho}{\mu}\int_{a_1}^{a_2}\overline{u_r' u_z'}\,dr}{2\ln\left\{\frac{a_2}{a_1}\right\}} - \frac{\rho}{\mu(a_2^2 - a_1^2)}\int_{a_1}^{a_2}\overline{u_r' u_z'}\,r^2 dr. \quad (40)$$

An overall force balance indicates that the mean shear stress on the two walls, τ_{wm}, is related to the pressure gradient as follows:

$$\tau_{wm} \equiv \frac{a_1\tau_{w1} + a_2\tau_{w2}}{a_1 + a_2} = \frac{a_2 - a_1}{2}\left(-\frac{\partial P}{\partial z}\right). \quad (41)$$

Introducing this quantity as well as $Re \equiv [2(a_2 - a_1)u_m\rho]/\mu$, $f_m \equiv (2\tau_{wm}/\rho u_m^2)$, $\phi_m^+ = (\rho\overline{u_r' u_z'})/\tau_{wm}$, and $\lambda = a_1/a_2$ allows Eq. 40 to be expressed in the dimensionless form

$$f_m\,Re = \frac{16(1-\lambda)^2}{1 + \lambda^2 - \frac{1-\lambda^2}{\ln\left\{\frac{1}{\lambda}\right\}} + \frac{2(1-\lambda)\int_\lambda^1 \phi_m^+ d\left(\frac{r}{a_2}\right)}{\ln\left\{\frac{1}{\lambda}\right\}} - \frac{4}{3(1-\lambda)}\int_\lambda^1 \phi_m^+ d\left(\frac{r}{a_2}\right)^3}. \quad (42)$$

The following supplemental expressions are also useful in interpreting the behavior of the total shear stress in annular flow. Making a force balance between any r and $r = a_0$, the radius of zero total shear stress, gives

$$\tau = \frac{a_0^2 - r^2}{2r}\left(-\frac{\partial P}{\partial z}\right). \quad (43)$$

The total local shear stress is seen from Eq. 43 to be positive for $a_1 \le r < a_0$ and negative for $a_0 < r \le a_2$. (Negative values of τ occur for parallel plates for $b < y < 2b$ as implied by Eq. 8, but that result is only an artifact of the definition of v' with respect to the wall at $y = 0$ rather than with respect to the absolute distance from the central plane.) The dependence of τ on r in annuli is seen to be bilinear as contrasted with the simple linear dependence for round tubes and parallel plates.

Specializing Eq. 43 for $r = a_1$ gives

$$\tau_{w1} \equiv \tau_{r=a_1} = \frac{a_0^2 - a_1^2}{2a_1}\left(-\frac{dP}{dz}\right) \quad (44)$$

from which it follows that

$$\frac{\tau}{\tau_{w1}} = \left(\frac{a_0^2 - r^2}{a_0^2 - a_1^2}\right)\frac{a_1}{r}. \quad (45)$$

Specializing Eq. 43 for $r = a_2$ instead gives

$$\tau_{w2} \equiv -\tau_{r=a_2} = \frac{a_2^2 - a_0^2}{2a_2}\left(-\frac{dP}{dz}\right) \quad (46)$$

and

$$-\frac{\tau}{\tau_{w2}} = \left(\frac{r^2 - a_0^2}{a_2^2 - a_0^2}\right)\frac{a_2}{r}. \quad (47)$$

It follows that

$$\frac{\tau_{w1}}{\tau_{w2}} = \left(\frac{a_0^2 - a_1^2}{a_2^2 - a_0^2}\right)\frac{a_2}{a_1}. \quad (48)$$

Here, τ_{w2} was arbitrarily defined so as to have the same sign as τ_{w1}.

Experimental and theoretical confirmation

Kjellström and Hedberg (1966) derived the equivalent of Eqs. 31, 35, 36, and 40, and attempted to test experimentally the implication of a difference between a_0 and a_{max} by measuring the pressure gradient and the radial distributions of u and $\overline{u_r' u_z'}$ for several aspect ratios. The differences between the values determined for a_0 and a_{max} were within the range of the experimental uncertainty of these locations for smooth annuli, but proved to be distinguishable for annuli with one rough and one smooth surface.

Lawn and Elliott (1972) did succeed in determining distinct values for a_0 and a_{max} for smooth annuli. They located the zero in the total shear stress both by hot-wire anemometry and by a sliding-sleeve technique, and the zero in the gradient of the time-mean velocity by two slightly displaced Pitot tubes as well as by graphically differentiating velocities measured with a single Pitot tube. A definite outward displacement of a_{max} relative to a_0 was noted. The displacement increases with decreasing aspect ratio, λ, but appears to be independent of *Re* over the fairly limited range of these experiments. Rehme (1974) subsequently carried out similar experiments, encompassing even smaller values of λ, and confirmed distinct locations for a_0 and a_{max}.

During essentially the same period of time, Hanjalić and Launder (1972b) carried out finite-difference calculations using a $k - \epsilon - \overline{u'v'}$ model for $Re = 2.4 \times 10^5$ in an annulus with $\lambda = 0.088$ (to match one of the experiments of Lawn and Elliott). Their computed velocities agree closely with the experimental ones, and together with the computed shear stress clearly identify separate locations for a_0 and a_{max}.

Rehme (1974) correlated his own experimental data for a_0, as well as that of Lawn and Elliott (1972), Kjellström and Hedberg (1966), and others, at $Re \cong 10^5$ with the expression

$$\frac{a_0 - a_1}{a_2 - a_0} = \lambda^{0.386}, \tag{49}$$

whereas Kays and Leung (1963) earlier correlated various data for a_{max} by

$$\frac{a_{max} - a_1}{a_2 - a_{max}} = \lambda^{0.343}. \tag{50}$$

Equations 49 and 50 can be combined to obtain

$$\frac{a_{max} - a_0}{a_2 - a_1} = \frac{\lambda^{0.343} - \lambda^{0.386}}{(1+\lambda^{0.343})(1+\lambda^{0.386})}. \tag{51}$$

The fractional difference in $a_{max} - a_0$ as represented by Eq. 51 is only 2.6% at $\lambda = 0.01$. However, the corresponding error in τ_{w1} as calculated from Eq. 44 using a_{max} instead of a_0 is 37%. The error due to assuming that $a_{max} = a_0 = (a_0)_{lam}$ is 3.8% of $a_0 - a_1$ at $\lambda = 0.5$ and the corresponding error in τ_{w1} is 10.3%. For $\lambda = 0.01$ these errors increase to 17.8% and 364%, respectively.

Interpretation

The variation in u, $-\rho\overline{u_r'u_z'}$, and τ across the annulus, based on the preceding expression and the available experimental data and numerical solutions, is shown in Figure 3. The turbulent shear stress $-\rho\overline{u_r'u_z'}$, as represented by the dashed curve, is positive from $r = a$, up to nearly $r = a_0$ and negative for all higher values of r. This quantity is of course equal to the total shear stress at $r = a_{max}$ and actually greater in absolute value from r slightly less than a_0 up to a_{max} because the viscous and turbulent shear stresses act in opposite directions in that interval.

Although Eqs. 39 and 40 are more complicated than the corresponding expressions for parallel plates and round tubes owing to the nonlinear variation of the total shear stress and the presence of the parameter λ, the contribution of the fluctuating components of the velocity can again be seen to be additive algebraically.

The additional and even more important contribution of the integral formulation in this geometry is the purely formal prediction of a difference in the locations of the maximum in the velocity and the zero in the total shear stress. The consequences of this difference will now be examined.

For flow in a round tube or between parallel plates, the shear stress on the wall, and hence the variation of the total shear stress across the channel, can be determined from measurements of the pressure gradient alone. However, for an annulus, as indicated by Eqs. 44 and 46, the shear stress on one of the walls or the location of the zero in the shear stress must in addition be determined in order to define the radial variation of the total shear stress. In most experimental investigations a_{max} has been evaluated (with great uncertainty) from the velocity distribution and inferred to equal a_0. In many instances the further error has been made of using the

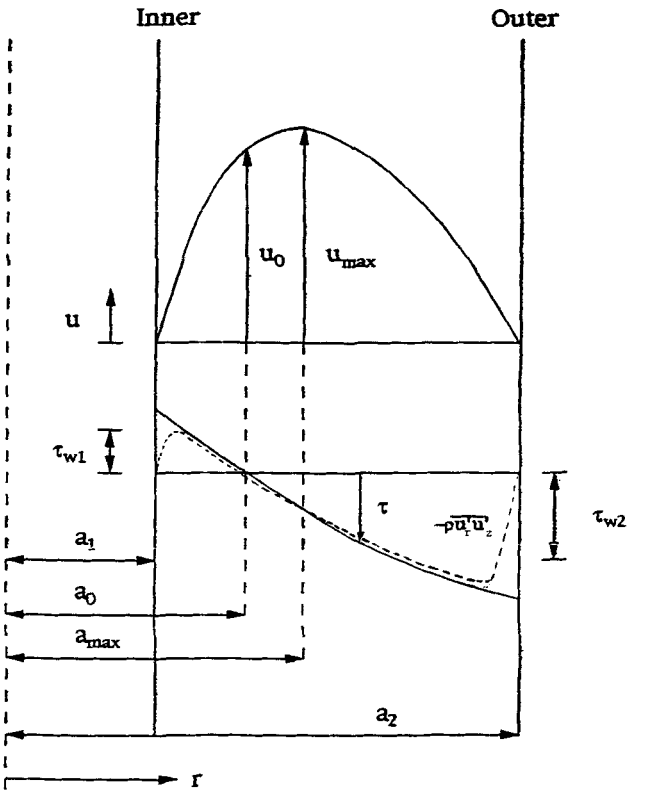

Figure 3. Velocity, total shear stress, and turbulent shear stress in an annulus.

theoretical value of a_{max} for laminar flow as an approximation for both a_{max} and a_0 in turbulent flow. As a consequence, virtually all of the values of τw_1 and τ_{w2} reported in the literature are subject to an unrecognized and unknown error that is difficult to correct retrospectively. This in turn leads to errors in plots and correlations for u^+ as a function of y^+ owing to the incorporation of τ_{w1} or τ_{w2} in both of these dimensionless variables. Rehme (1974) demonstrated that improved correlations of $u^+\{y^+\}$ could be attained from the data of earlier investigators by utilizing a_0 from Eq. 49 to determine τ_{w1} and τ_{w2} rather than the original values of a_0 that were taken as equivalent to a_{max}.

The use of a_{max} for a_0 has also been incorporated unwittingly in virtually all of the many semitheoretical solutions that employ velocity distributions adapted from those for round tubes or parallel plates and then match the velocities for the inner and outer regions at $r = a_{max} = a_0$. The futility of the latter step is apparent from Figure 3.

In keeping with Eq. 33, the eddy viscosity for an annulus is defined as

$$\mu_t = \frac{-\rho\overline{u_r'u_z'}}{du/dr}. \tag{52}$$

From Figure 3, this quantity can be inferred to be positive for $r > a_{max}$, unbounded (infinite) for $r = a_{max}$, negative for $a_0 < r < a_{max}$, zero for some value of r slightly less than a_0, and positive again for r less than that value. Obviously, the eddy viscosity concept is not truly applicable for an annulus. The

$k-\epsilon$ model, which functions by generating the eddy viscosity, is also precluded. The mixing length concept is subject to similar anomalies. Maubach and Rehme (1972) apparently first noted such discrepancies in the eddy viscosity in connection with flow between one rough and one smooth parallel plate. These shortcomings were, however, not recognized by earlier experimenters who determined the eddy viscosity or mixing length for annuli, or by analysts who utilized such quantities.

The overall friction factor defined above Eq. 42 does not involve a_0 and hence is not subject to error arising from the misdetermination of that quantity. However, separate friction factors have often been defined and determined for the inner $(a_1 < r < a_0)$ and outer $(a_0 < r < a_2)$ regions in the expectation of greater similarity of their functional dependence on the Reynolds number to that for parallel plates and round tubes. These separate friction factors are impacted by the determination of a_0 and thereby of τ_{w1} and τ_{w2}. A further complication arises if they are based on the mean flow in the subregions since that partitioning depends on a_0 and the corresponding velocity distributions as sketched in Figure 3.

Why have not the discrepancies in experimental correlations and semitheoretical solutions that result from using a_{max} or $(a_0)_{lam}$ for a_0 been recognized? First, most experimental investigations have been for aspect ratios approaching unity, for which the effects are small and perhaps even tolerable. Second, the effects when small have often been overshadowed by experimental error; this is particularly true with sensitive quantities such as the eddy viscosity that depend on derivatives. In results obtained by semitheoretical modeling, any overt evidence of anomalous behavior is precluded by the inherent postulate of $a_0 = a_{max}$. Also, disparity with experimental results is often disguised by the adjustment of empirical coefficients.

Other Geometries and Conditions

It may be inferred from derivations similar to those for smooth annuli that in turbulent flow the maximum in the velocity and the zero in the shear stress will occur at different locations for all conditions and geometries for which the shear stress is unequal on opposing surface. Such conditions include concentric circular annuli and one rough and one smooth surface, as well as two surfaces of unequal roughness, for parallel plates. The combination of forced and induced (Poiseuille and Couette) flow is another such condition. Geometries that produce an equal shear stress on opposing surfaces include all open channels, many two-dimensional channels such as trapezoids, and all curved channels. (In two-dimensional and curved channels a secondary motion is an added and perhaps even greater complication.)

Experimental and theoretical results for the separate locations of the maximum in the velocity and the zero in the total shear stress are very limited for these other conditions and geometries. Values of a_0 and a_{max} for annuli with one smooth and one rough surface were determined experimentally by Kjellström and Hedberg (1966), and computationally by Hanjalić and Launder (1972b). Although Wilke et al. (1967) did not determine the location of the zero in the shear stress in their experiments with one smooth and one rough plate, they concluded retrospectively that the failure to do so was the source of the obvious discrepancies in their correlations for such data. Determinations of separate locations for the zero in the shear stress and the maximum in the velocity were accomplished for one rough and one smooth plate by Maubach and Rehme (1972) experimentally and by Hanjalić and Launder (1972a) computationally. Maubach and Rehme attempted, without great success, to construct a general correlation for the location of the zero in the shear stress as a function of the location of the maximum in the velocity for both parallel plates and annuli with both smooth and nonidentical surfaces.

Summary and Conclusions

Formal integration of the time-averaged equations of conservation for fully developed, fully turbulent flow in channels has been shown earlier to provide considerable insight on the functional behavior. Such formulations are exact in every sense and relatively simple. They can be used with an empirical correlation such as Eq. 17 to provide detailed quantitative results, but their primary value is perhaps qualitative. They provide a guideline for both experimentation and analysis that has generally been overlooked. This oversight has had serious consequences including the publication of erroneous results, both experimental and analytical, in particular for annuli.

For the simplest of all channels, that formed by two, smooth parallel plates, a first integration reveals that (1) the cross-product $\overline{v'w'}$ is zero everywhere; (2) the pressure within the channel is equal to that at the wall minus the local value of $\rho\overline{v'v'}$; and (3) the turbulent shear stress $-\rho\overline{u'v'}$ vanishes at the midplane as well as at the wall. A second integration of the equation for the conservation of momentum in the direction of flow produces a formal expression for the local time-mean velocity that consists of the algebraic sum of the well-known terms for purely laminar flow and a simple integral of $\rho\overline{u'v'}/\tau_w$. The corresponding formal expression for the space-mean velocity, and thereby for the friction factor, can be reduced to the algebraic sum of the well-known term for laminar flow and a weighted integral of $\rho\overline{u'v'}/\tau_w$.

Similar results are obtained for a round tube despite the slight complication arising from curvature and the presence of a centrifugal force.

Similar results are also obtained for a concentric circular annulus, but with further effects of curvature. More importantly, a first integral of the equation of conservation for the direction normal to the wall reveals that for turbulent flow the locations of the maximum in the velocity and the zero in the total shear stress differ in this geometry. That result, which is represented most simply by Eq. 26, is in contrast with the occurrence of zero turbulent shear stress at the midplane of smooth parallel plates and the centerline of round tubes.

The difference in the locations of the maximum in the velocity and the zero in the shear stress for annuli has several important consequences. First, the evaluation of a_0 requires the experimental determination of τ_{w1} or τ_{w2} in addition to the pressure gradient (Eqs. 44 and 46). Second, the use of a_{max} in place of a_0 results in even greater percentage errors in the corresponding values determined for τ_{w1} and τ_{w2}. These errors are incorporated in the values of both u^+ and y^+. Third, the noncoincidence of a_0 and a_{max} results in an un-

bounded value for the eddy viscosity at a_{max} and negative values extending from a_{max} to a value of r slightly less than a_0. Thus, the concept of the eddy viscosity is inapplicable to annuli, at least in that region. The $k-\epsilon$ model for turbulence, which functions by generating an eddy viscosity, is correspondingly excluded. The mixing-length concept suffers from related shortcomings. Some more complex models for turbulent flow, such as those based on the Reynolds stresses, remain valid. A fourth, more subtle consequence of the noncoincidence of a_0 and a_{max}, but one apparent from Figure 3, is that the many solutions for annuli based on the matching at a_0 of velocity distributions adapted from parallel plates or round tubes are invalid. Fifth, although the overall friction factor defined in terms of τ_{wm} and u_m is not dependent on a_0, the separate friction factors for the inner and outer surfaces of the annulus are directly dependent on a_0 through τ_{w1} and τ_{w2}, and, secondarily as well if based on the mean velocities in the inner and outer region.

The difference between a_0 and a_{max} in annuli is small except for very small λ, but the resulting errors in τ_{w1} and τ_{w2} are percentagewise much greater. The errors due to postulating $a_0 = a_{max} = (a_0)_{lam}$ are even greater. For the usual practical case of λ approaching unity, all of the errors and effects mentioned earlier may be tolerable. This is the explanation for the failure of most experimentalists to note anomalies associated with the use of a_{max} or even $(a_{max})_{lam}$ for a_0.

A difference between the locations of the maximum in the velocity and the zero in the shear stress occurs in any geometry and for any condition that gives rise to a nonequality of the shear stress on an opposing surface. The consequences previously enumerated for annuli are then applicable in varying degrees.

Notation

a = radius of round tube or annulus, m
a^+ = dimensionless radius $= [a(\tau_w \rho)^{1/2}]/\mu$
A_x = cross-sectional area, m^2
b = half-spacing of parallel plates, m
b^+ = dimensionless half-spacing, $= [b(\tau_w \rho)^{1/2}]/\mu$
f = Fanning friction factor $= 2\tau_w/\rho u_m^2$
f_m = overall Fanning friction factor for an annulus $= 2\tau_{wm}/\rho u_m^2$
l = mixing length, m
L = wetted perimeter, m
P = time-averaged dynamic pressure, Pa
r = radial coordinate, m
u = time-averaged velocity in direction of flow, m/s
u' = fluctuating component of velocity in principal direction of flow, m/s
u'_r = fluctuating component of velocity in radial direction in polar coordinates, m/s
u'_θ = fluctuating component of velocity in tangential direction in polar coordinates, m/s
u'_z = fluctuating component of velocity in principal direction of flow in polar coordinates, m/s
u^+ = dimensionless velocity $= u(\rho/\tau_w)^{1/2}$
v' = fluctuating component of velocity in y direction, m/s
w' = fluctuating component of velocity in direction of unbounded breadth for parallel plates, m/s
x = distance in principal direction of flow for parallel plates, m
y = distance from the lower wall, m
y^+ = dimensionless distance $= [y(\tau_w \rho)^{1/2}]/\mu$
z = distance in principal direction of flow for round tubes and annuli

Greek letters

λ = aspect ratio $= a_1/a_2$
μ = dynamic viscosity, Pa·s
ν = kinematic viscosity, m^2/s
ϕ^+ = dimensionless turbulent shear stress $= -\rho\overline{u'v'}/\tau_w$ or $\rho\overline{u'_r u'_z}/\tau_w$

Subscripts

1 = on inner wall of annulus
2 = on outer wall of annulus
a = at $r = 0$
b = at $y = b$

Literature Cited

Boussinesq, J. "Essai sur la Théorie des Eaux Courantes," *Mém. présentes par divers savants á l'Académie des Sciences de l'Institut de France*, **23**, Paris, p. 1 (1877).

Churchill, S. W., *The Interpretation and Use of Rate Data: The Rate Process Concept*, rev. printing, Hemisphere, Washington, DC (1979).

Churchill, S. W., "New and Overlooked Relationships for Turbulent Flow in Channels," *Chem. Eng. Technol.*, **13**, 264 (1990).

Churchill, S. W., and C. Chan, "Theoretically Based Correlating Equations for the Local Characteristics of Fully Turbulent Flow in Round Tubes and between Parallel Plates," *Ind. Eng. Chem. Res.*, **34**, 1332 (1995).

Churchill, S. W., *Turbulent Flows. The Practical Use of Theory*, Notes, Univ. of Pennsylvania, Philadelphia (1994).

de Nevers, N., "Rate Data and Derivatives," *AIChE J.*, **12**, 110 (1966).

Hanjalić, K., and B. E. Launder, "Fully Developed Axisymmetric Flow in a Plane Channel," *J. Fluid Mech.*, **51**, 301 (1972a).

Hanjalić, K., and B. E. Launder, "A Reynolds Stress Model of Turbulence and Its Application to Thin Shear Flows," *J. Fluid Mech.*, **53**, 609 (1972b).

Kampe de Fériet, J., "Sur l'Écoulement d'un Fluide Visqueux Incompressible entre Deux Plaques Paralléles Indéfinies," *Houille Blanche*, **3**, 509 (Nov.–Dec., 1948).

Kays, W. M., and E. Y. Leung, "Heat Transfer in Annular Passages —Hydrodynamically Developed Turbulent Flow with Arbitrarily Prescribed Heat Flux," *Int. J. Heat Mass Transfer*, **6**, 537 (1963).

Kim, J., P. Moin, and R. Moser, "Turbulence Statistics in Fully Developed Channel Flow at Low Reynolds Numbers," *J. Fluid Mech.*, **177**, 133 (1987).

Kjellström, B., and S. Hedberg, *On Shear Stress Distributions for Flow in Smooth or Partially Rough Annuli*, Aktiebolaget Atomenergi Rep. AE-243, Stockholm (1966).

Laufer, J., *Investigation of Turbulent Flow in a Two-Dimensional Channel*, NACA Rep. 1053, Washington, DC (1951).

Lawn, C. J., and C. J. Elliott, "Fully Developed Turbulent Flow through Concentric Annuli," *J. Mech. Eng. Sci.*, **14**, 195 (1972).

Lyons, S. L., T. J. Hanratty, and J. B. McLaughlin, "Large-Scale Computer Simulation of Fully Developed Channel Flow with Heat Transfer," *J. Num. Methods Fluids*, **13**, 999 (1991).

Maubach, K., and K. Rehme, "Negative Eddy Diffusivities for Axisymmetric Turbulent Velocity Profiles," *Int. J. Heat Mass Transfer*, **15**, 425 (1972).

Pai, S. I., "On Turbulent Flow between Parallel Plates," *J. Appl. Mech.*, **20**, 109 (1953a).

Pai, S. I., "On Turbulent Flow in Circular Pipe," *J. Franklin Inst.*, **256**, 337 (1953b).

Prandtl, L., "Bericht über Untersuchungen zur ausgebildeten Turbulenz," *Z. Angew. Math. Mech.*, **5**, 136 (1925).

Rehme, K., "Turbulent Flow in Smooth Concentric Annuli with Small Radius Ratios," *J. Fluid Mech.*, **64**, 263 (1974).

Rutledge, J., and C. A. Sleicher, "Direct Simulation of Turbulent Flow and Heat Transfer in a Channel: 2. Smooth Walls," *Int. J. Num. Methods Fluids*, **6**, 1051 (1993); also see Rutledge, J., "Direct Simulation of Enhancement of Turbulent Heat Transfer by Micro-Riblets," PhD Thesis, Univ. of Washington, Seattle (1988).

Wilke, D., M. Cowin, R. Burnett, and T. Burgoyne, "Friction Factor Measurements in a Rectangular Channel with Walls of Identical and Non-Identical Roughness," *Int. J. Heat Mass Transfer*, **10**, 611 (1967).

Manuscript received July 28, 1994, and revision received Dec. 27, 1994.